ENGINEERING REPORT NO. ___9149___ _____

OPTICAL DESIGN OF A TWO-ELEMENT

ECHELLE SPECTROGRAPH

DATE: 22 January 1968

PERKIN-ELMER

PERKIN-ELMER

OPTICAL GROUP   NORWALK, CONNECTICUT

ENGINEERING REPORT NO. ___9149___

OPTICAL DESIGN OF A TWO-ELEMENT
ECHELLE SPECTROGRAPH

DATE: 22 January 1968

PREPARED FOR: PRINCETON UNIVERSITY

OBSERVATORY

(NASA CONTRACT NO. NGR-31-001-044)

_____

PREPARED BY: _D.A. Markle_

D.A. Markle

APPROVED BY: _Alan B. Wissinger_

Alan B. Wissinger

H.S. Hemstreet

H.S. Hemstreet

PERKIN-ELMER

TABLE OF CONTENTS

LIST OF ILLUSTRATIONS

SECTION I

INTRODUCTION

In March 1965 Perkin-Elmer was awarded a NASA funded feasibility study program by Princeton University Observatory. One of the main purposes of the study was to design a very compact telescope system having a 40-inch-diameter aperture and fitting within the 10-foot-long OAO spacecraft vehicle. The instrument section behind the telescope primary was to contain two SEC vidicon image tubes, either of which would be used for diffraction-limited imagery or high resolution spectrophotometry. The spectrograph was envisaged as an echelle arrangement that would fold the spectrum like the lines of type on a printed page thereby permitting a very large wavelength increment to be integrated by the vidicon between each readout. Several echelle spectrograph arrangements were found that could be packaged within the narrow confines of the instrument section. All of the spectrograph arrangements employed two mirrors and two gratings except for one which consisted of only two gratings. The reduced number of optical surfaces in the latter scheme appeared to offer a factor of 4 greater efficiency in the far UV where losses as high as 50 percent per surface are common. .

In a subsequent phase of the Advanced Satellite Study (Perkin-Elmer Engineering Report No. 8585) the aberrations of the two-element spectrograph were studied using an analytical technique permitting paper-and-pencil analysis. This indicated that a two-element system was feasible; but,

1

because of the large number of aberrations inherent in such a system, an
independent check was deemed desirable.

In the present phase, the feasibility of a longer two-
element echelle was examined using a new optical design computer program and
a paper-and-pencil analysis similar to that used in the previous study. The
overall length of the spectrograph was increased since a new telescope vehicle
that permits a longer instrument package now appears likely, and because the
increased length would decrease the aberrations in such a system.

This report outlines the final spectrograph design parameters. The
balance of the effort under this contract will be to construct a breadboard
version of the spectrograph and measure the efficiency and scattering in the
far UV.

SECTION II

DESIGN DESCRIPTION

The final spectrograph design is shown in Figure 1 and the design parameters are listed in Table 1. The total distance between the f/10 focal plane and the center of the vidicon at the f/150 focal plane is approximately 750 mm (29.5 inches). The predisperser grating is a toroidal surface tilted slightly in the xz-plane and with its grating lines in the vertical or y-direction. The echelle is flat and tilted in the xy-plane so that the high dispersion direction is in the y-direction. The vidicon surface is at a compound angle with respect to the x-axis (telescope optical axis) and is displaced in the (minus) z-direction about 3 inches so that a wavelength of 1981Å is imaged in the center of the 35-mm-diameter vidicon format. It is essential that the separation between the vidicon and the telescope axis be at least 3 inches so that there is some clearance available between a pair of 5-inch-diameter vidicon tubes when they are arranged symmetrically about the telescope axis to provide redundancy. The direction cosines, $\cos\beta$ and $\cos\gamma$, listed at the bottom of Table 1 refer to the components of a unit vector normal to the vidicon surface when projected onto the y- and z-axes respectively. The relationship between the direction cosines and the angles shown in the top and side projections of Figure 1 is given by

$$\tan\beta' = \frac{\cos\beta}{\sqrt{1-\cos^2\beta-\cos^2\gamma}} \qquad (1)$$

TABLE I

PRINCETON ADVANCED SPECTROGRAPH
DESIGN PARAMETERS

Surface	f/10 Focal Plane	Predisperser	Echelle	Vidicon
Curvature	0.	$-0.0104219 \text{mm}^{-1}$ *	0	0
Separation	51.4286mm	−36.429mm	734.465mm	-
Grating Spacing	-	180/mm	160/mm	-
y Decenter	0.	0.	0.	0.
z Decenter	0.	0.	0.	−75.76mm
$\cos\beta$	0.	0.	0.31846	−0.524
$\cos\gamma$	0.	0.0310802	0.	0.200

*Toroidal surface with major and minor axes rotated 45° with respect to
to the yz-axis. Curvatures of major and minor axes equal -0.0104219 and
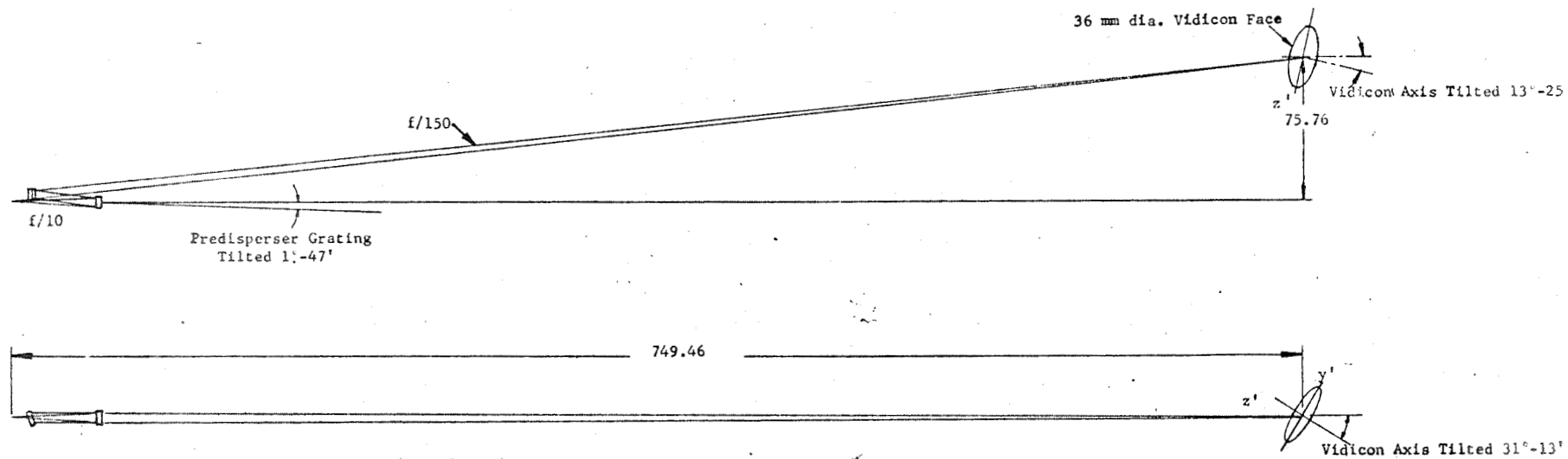-0.0103410, respectively.

36 mm dia. Vidicon Face

Vidicon Axis Tilted 13°-25

f/150

z'

75.76

f/10

Predisperser Grating
Tilted 1°-47'

749.46

y'

z'

Vidicon Axis Tilted 31°-13'

Figure 1. Princeton Advanced Satellite Spectrograph Layout

$$\tan\gamma' = \frac{\cos\gamma}{\sqrt{1-\cos^2\beta-\cos^2\gamma}} \qquad (2)$$

where β' is the projected angle in the xy-plane between the surface normal and the x-axis. γ' is the projected angle in the xz-plane between the surface normal and the x-axis.

Equations (1) and (2) are only required for compound angles. A simple tilt in either the β or γ direction, such as is the case with both gratings, can be shown directly on the usual orthogonal projections.

An enlarged view of the grating elements is shown in Figure 2. The predisperser is only about 6 mm in diameter and the echelle is about 7 mm square. At the central design wavelength of 1981Å there is a small separation between the incoming f/10 beam and the f/150 predisperser beam at the echelle grating. At 1000Å the two beams overlap slightly. The overlap could be avoided by moving the vidicon further away from the optical axis but only at the cost of increasing the amount of coma and increasing the tilt between the vidicon axis and the telescope axis. If a small groove is ground in the side of the echelle to pass the f/10 beam and if the edge of the echelle is positioned to catch all the predisperser beam except for the portion hitting the groove, then the amount of vignetting is negligibly small at 1000Å and approaches zero at 1500Å. The maximum amount of vignetting is illustrated in Section A-A of Figure 2.

Also shown in the end view of Figure 2 is the axes of the toroidal surface on the predisperser grating. The actual amount of aspherizing can be computed as follows:
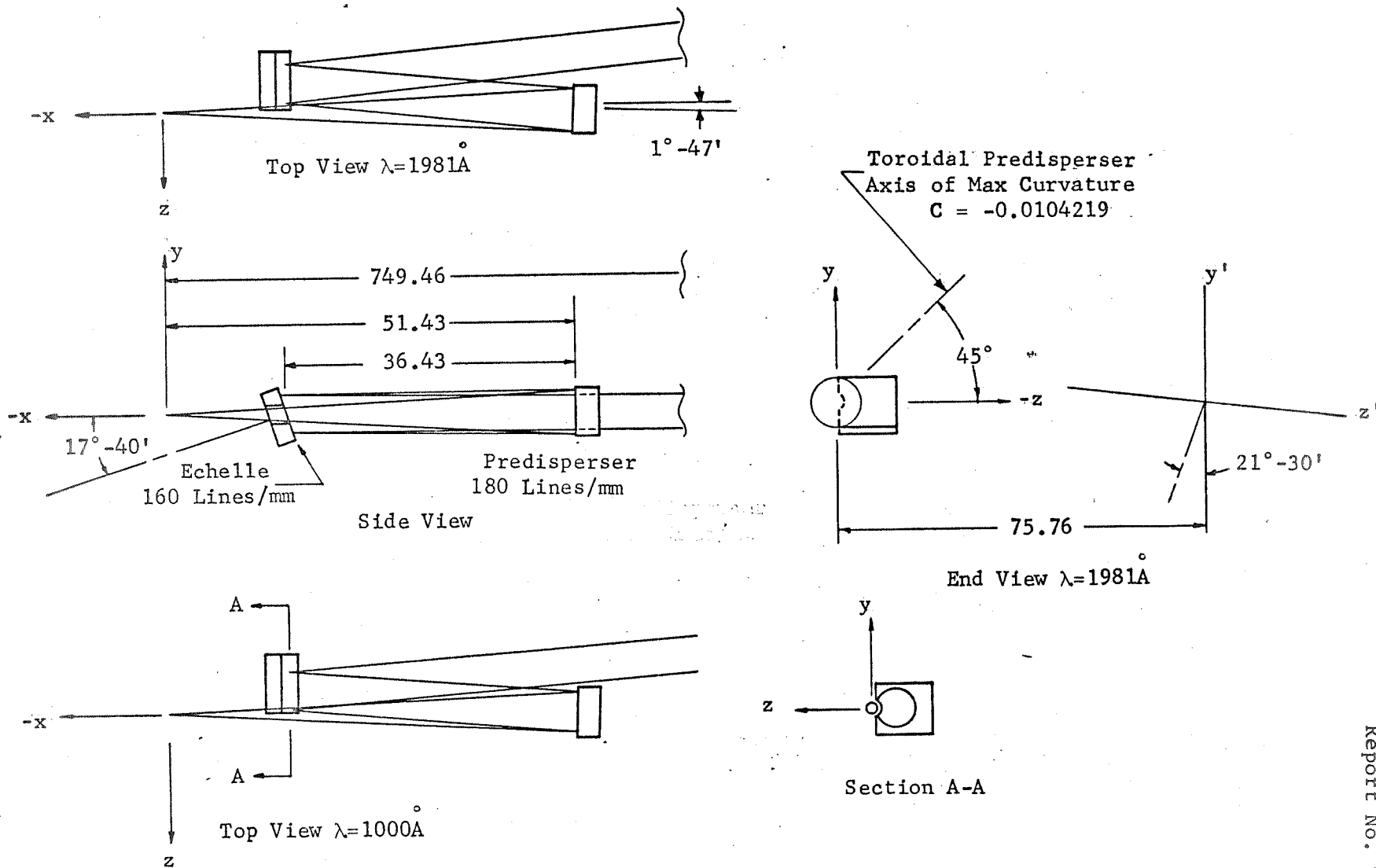
6

Top View λ=1981Å

1°-47'

Toroidal Predisperser
Axis of Max Curvature
C = -0.0104219

y

749.46

51.43

36.43

-x

17°-40'

Echelle
160 Lines/mm

Predisperser
180 Lines/mm

Side View

45°

-z

y'

z'

21°-30'

75.76

End View λ=1981Å

A

A

A

-x

z

y

z

Section A-A

Top View λ=1000Å

Figure 2. Princeton Advanced Satellite Spectrograph Design Details

$$\Delta S = \frac{x^2}{4} (C_1 - C_2) \tag{3}$$

where ΔS is the maximum difference in sag between two points equidistant from the center of the toroid; x is the radius from the center; and C_1 and C_2 are the maximum and minimum curvatures on the toroid. Substituting into (3) we get:

$$\Delta S = \frac{1}{4} \left(\frac{5.143}{2}\right)^2 \left(0.0104219 - 0.0103410\right)$$

$$= (1.65)(0.0000809)$$

$$= 0.134 \text{ micron}$$

$$\approx \lambda/4$$

This is not an inordinate amount of aspherizing but, because it is applied to a reflective surface, it has twice this effect on the optical path.

The relationship between the orthogonal coordinate system x,y,z, that is tied to the telescope axis and the high and low grating dispersion directions, and the orthogonal coordinate system used to reference positions on the vidicon surface y',z' is shown in Figure 1. The order of operations performed by the computer is such that the tilted y'-axis lies in the xy-plane but the x'-axis is skewed with respect to the xyz-axis. Thus the high resolution direction corresponds to the y- or y'-axis but the low resolution direction corresponding to the x-axis appears skewed on the vidicon format.

The format details are shown in Figure 3. Each line corresponds to a different order of interference on the echelle grating. Thus 2824Å
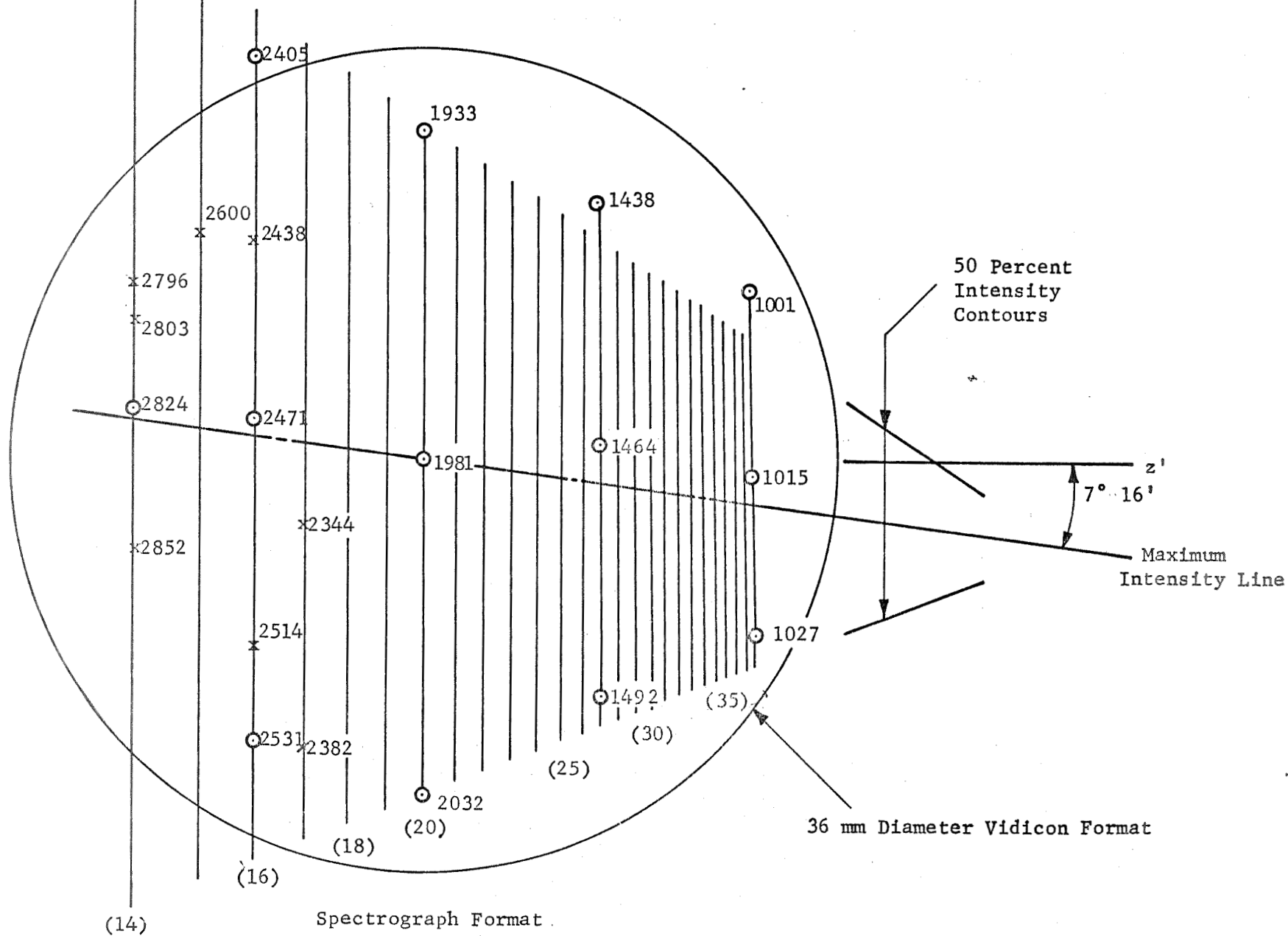
9

2405

1933

2600
2438

50 Percent
Intensity
Contours

2796

2803

1001

2824

2471

z'

1981

1464

7° 16'

1015

2344

Maximum
Intensity Line

2852

2514

1027

2531 2382

1492

(35)

(30)

(25)

2032

(20)

(18)

36 mm Diameter Vidicon Format

(16)

(14)

Spectrograph Format

Figure 3. Princeton Advanced Satellite Spectrograph Format

occurs at the 14th order and $1015\overset{\circ}{\text{A}}$ occurs at the 39th order. The center

wavelength of each line is approximated by

$$\lambda_c = \frac{39620}{m} \quad \text{angstroms} \tag{4}$$

where m is the order of interference at the echelle. The wavelength range

covered by each line between the 50-percent points is approximately

$$\Delta\lambda = \frac{39620}{m^2} \quad \text{angstroms} \tag{5}$$

The reciprocal dispersion in angstroms per millimeter is approximately:

$$\frac{1}{D} = 1.72 \times 10^{-3}\lambda \tag{6}$$

when λ is in angstroms.

Thus at $1000\overset{\circ}{\text{A}}$ the scale is 1.72 $\overset{\circ}{\text{A}}$/mm and at $2000\overset{\circ}{\text{A}}$ it is 3.44

$\overset{\circ}{\text{A}}$/mm, etc.

When viewed along the vidicon axis the xz-plane intersects the

vidicon surface at an angle of $7°-16'$ because of the compound angle between

the vidicon axis and the x,y,z axis. Since this also corresponds to the

maximum intensity diffraction direction, the format is similarly tipped.

The amount of tipping is a function of the product of the two direction

cosines, $\cos\beta$ and $\cos\gamma$. If $\cos\beta$ and $\cos\gamma$ are left unrestricted except for

determining the optimum focal position, the amount of tipping becomes

inconveniently large (greater than $15°$). Therefore, it was found preferable

to set $\cos\gamma$ to a convenient value and thereby limit the amount of tipping at

the expense of somewhat less than optimum focus across the format.

Because of the awkward trapezoidal shape of the spectrograph
format, it was desirable to knock off a few corners rather than reduce the
dispersion. However a number of wavelengths corresponding to interstellar
absorption lines were randomly positioned throughout the spectrum and it
was undesirable to knock out any of these.

A number of formats were tried before one was found in which all
of the desired wavelengths fell within the 36-mm-diameter vidicon surface.
The desired wavelengths are indicated by x in Figure 3. The wavelengths
marked o were used to determine the aberrations at various points in the
format.

SECTION III

GEOMETRICAL ABERRATIONS

The aberrations of the spectrograph were studied using a computer program which performed a geometrically exact ray trace. Representative points in the format were examined using fans of rays in both y- and z-directions, each of which consisted of seven equally spaced rays spanning the entrance aperture. Aberrations were computed by subtracting the coordinates of the two identical central rays from the corresponding coordinates of the other rays. In each case the skewed position of the focal plane was taken into account in computing the coordinates. The format positions of the various wavelengths used to study the aberrations are shown in Figure 3.

The y'- direction aberration (high resolution direction) for both y and z fans are illustrated in Figure 4. Across the center of the format (1933Å to 2032Å) the geometrical image size is less than 35 microns. At 2824Å this increases to a little over 40 microns, and at the other end of the spectrum (1015Å) the image size is about 85 microns. This compares favorably with a diffraction-limited image size of about 75 microns for 5000Å at f/150.

The z'-direction aberrations (low-resolution direction) for a few characteristic points are illustrated in Figure 5. These approach 200 microns in some places but, providing they do not cause adjacent lines to overlap in the spectrograph format, they do not adversely affect the vidicon resolution. Since the closest line spacing is about 400 microns, the z'- direction aberration size is well within bounds.
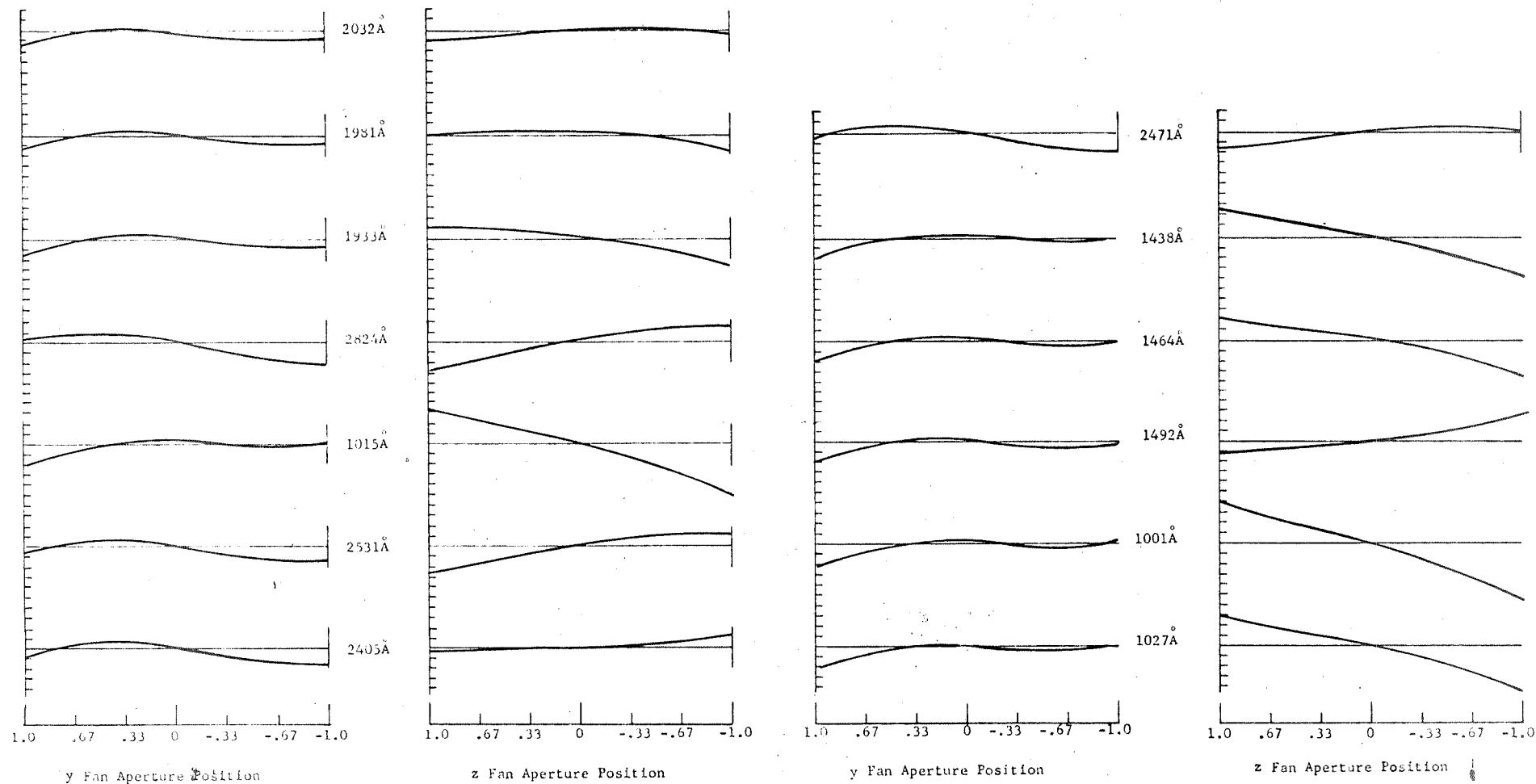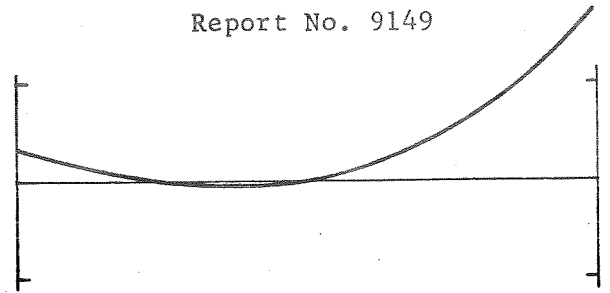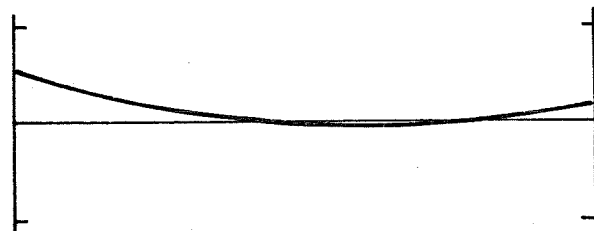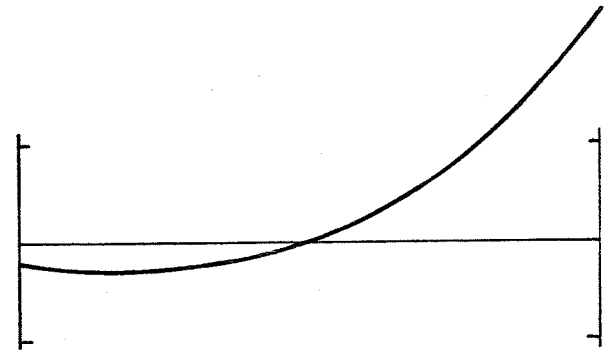
Figure 4. Aberration in y' Direction
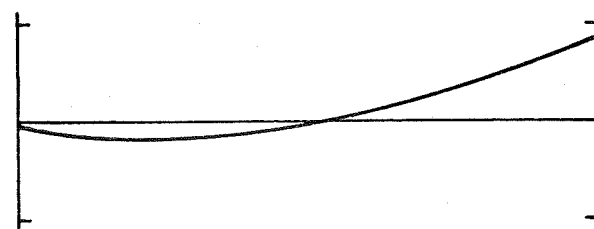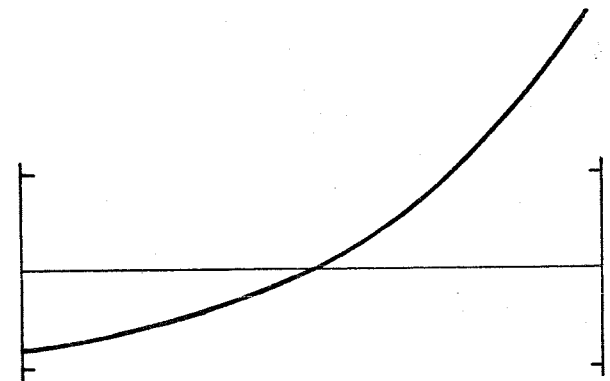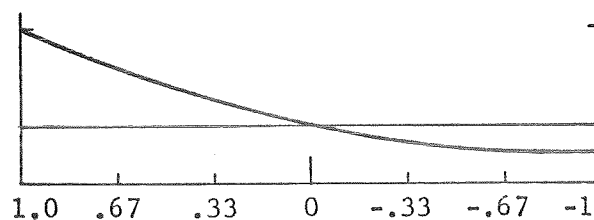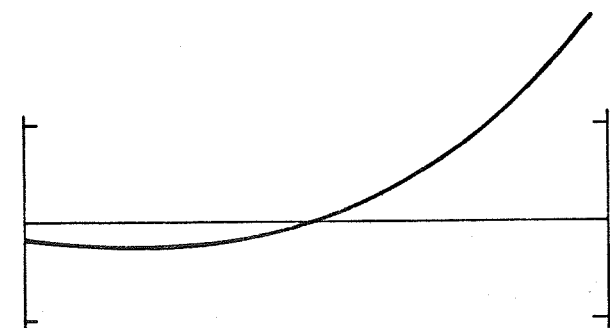(One Vertical Division Equals 10 Microns)
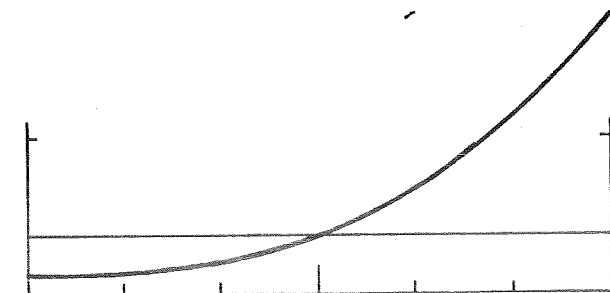
Figure 5. Aberrations in z' Direction
(One Vertical Division Equals 50 Microns)

14

As a check that nothing unusual was occurring in the spectrograph design, a second type of ray trace was performed. A total of eight rays spaced at 45-degree increments around the edge of the entrance pupil were traced through the system. Connecting the ray intercepts at the focal plane creates a Lissajous figure characteristic of the principal aberrations. The resulting pattern for five points in the spectrograph format and the entrance pupil coordinates of the eight rays are illustrated in Figure 6. The twisted ellipses are characteristic of coma and astigmatism. In general, the rim ray trace does predict an image size somewhat larger than predicted from the y and z ray fan traces. For example, at 1933Å and 2824Å the rim ray trace predicts an image size between 70 and 80 microns in the y-direction whereas the y and z fan traces indicated a size of only 35 or 40 microns. At the other end of the spectrum (1015Å), where the y and z fans indicated the relatively large image size of 85 microns, the agreement is quite good.

When the geometrical image size approaches the diffraction-limited image size, as it does in this case, then the interpretation of the image size can be misleading. For example, at f/150 a focal plane out of focus by 22.5 millimeters would cause a barely discernible image degradation, a maximum optical path difference of a quarter wavelength at 0.5 micron, and a geometrical image size of 150 microns. The relationship between geometrical image size and wavefront deformation is different for each type of aberration. However the comparable sizes of the geometrical and diffraction-limited images, together with analytically derived optical path differences, indicate that the spectrograph should operate very close to what would be expected from a diffraction-limited system.
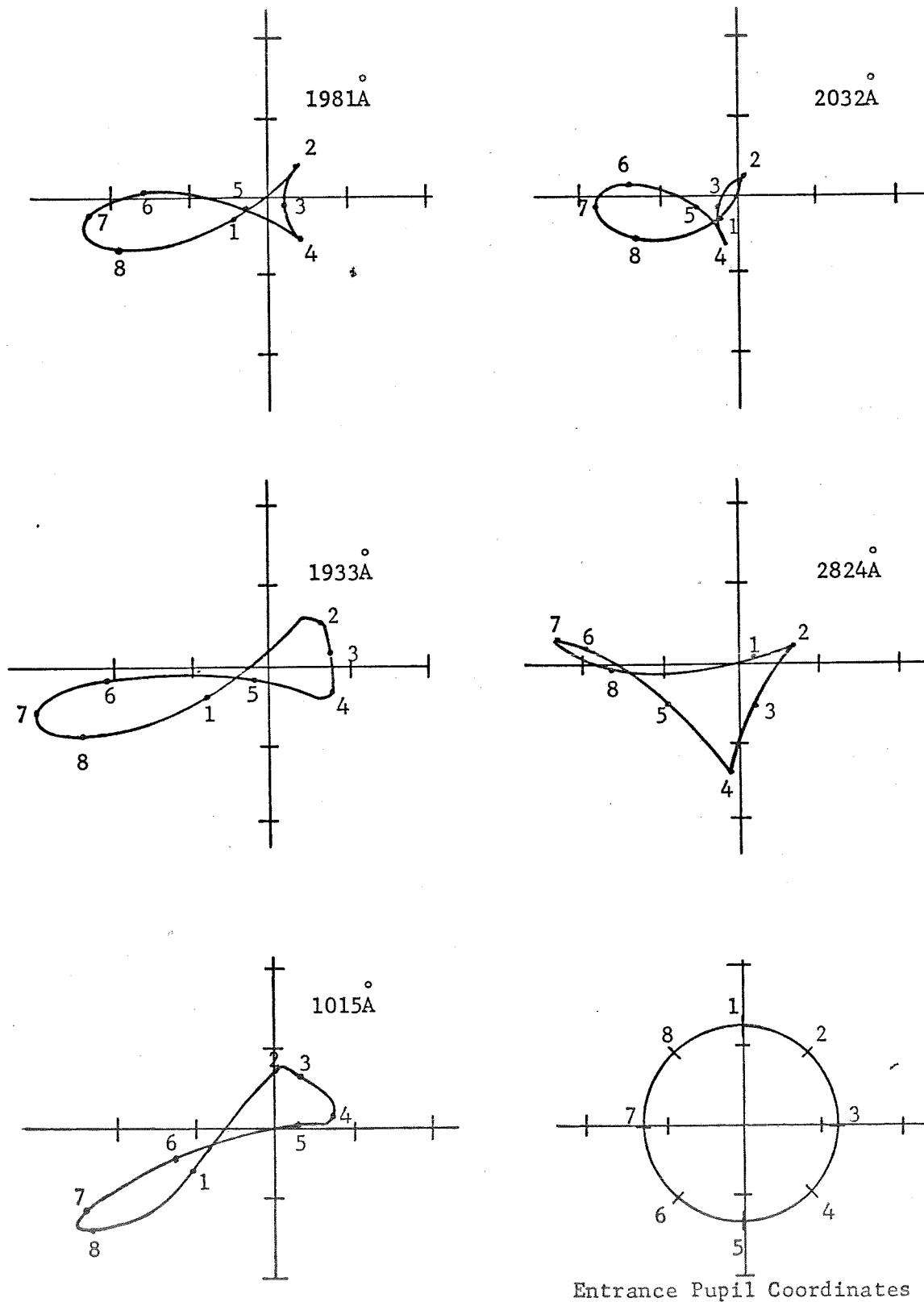
Figure 6. Rim Ray Trace Aberrations
(One Division equals 50 Microns)

16

SECTION IV

OPTICAL PATH DIFFERENCES

The usual method of dealing with aberrations is to expand the optical path between adjacent surfaces in a converging power series that includes the coordinates of the entrance pupil and the position of the object. If this is carried through to 3rd order, then individual surface contributions may be combined to obtain the total optical path differences (OPD's) present at the focal plane. A very similar technique can be applied to gratings[*] but the result is somewhat more complex because of the form of the grating equation and the general lack of rotational symmetry in grating systems.

For the present problem it is sufficient to consider only a single spherical grating acting as its own field stop. The geometry of such a system is illustrated in Figure 7. The x-axis is normal to the grating vertex and the two sets of orthogonal y-and z-axes contain the object and image points. The distance between a point y_1, z_1, and a point y_2, z_2 via the grating vertex is $r_1 + r_2$. For a generalized point on the grating surface (ξ, η) and a point x,y in an xy-plane a distance ℓ away from the grating, the path is given by:

$$P = \left[(\ell-\zeta)^2 + (y-\xi)^2 + (z-\eta)^2 \right]^{1/2} \tag{7}$$

where ζ is the sag of the spherical grating at the point ξ, η. If R is the radius of the grating, ζ is given by

---

[*] W. Werner, "The Geometrical Optical Aberration Theory of Diffraction Gratings", Applied Optics, Vol. 6, No. 10, p 1691.
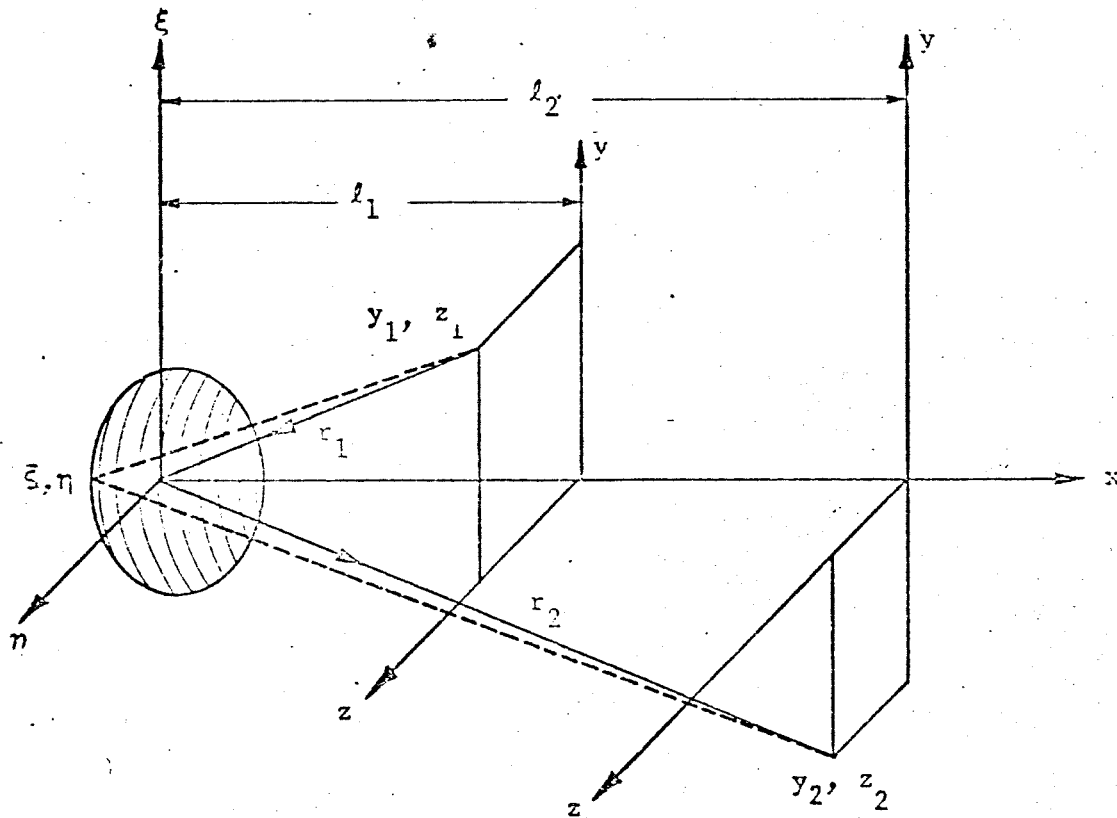
Figure 7. Grating Geometry

$$\zeta = \frac{\eta^2 + \xi^2}{2R} + \frac{(\eta^2 + \xi^2)^2}{8R^3} + \ldots \ldots \quad (8)$$

By definition

$$r^2 = \ell^2 + y^2 + z^2 \quad (9)$$

and

$$\ell = r\left(1 - \frac{y^2 + z^2}{r^2}\right)^{1/2} \quad (10)$$

$$\ell = r\left(1 - \frac{(y^2 + z^2)}{2r^2} - \frac{(y^2 + z^2)^2}{8r^4} + \ldots \ldots\right) \quad (11)$$

Substituting equations (8) and (11) into equation (7), we obtain

$$P = \left[r^2\left(1 - \frac{(y^2 + z^2)}{2r^2} - \frac{(y^2 + z^2)^2}{8r^4} - \frac{\eta^2 + \xi^2}{2Rr} - \frac{(\eta^2 + \xi^2)^2}{8rR^3}\right)^2 \right.$$
$$\left. + (y^2 + z^2) - 2(y\xi + z\eta) + (\xi^2 + \eta^2) \right]^{1/2} \quad (12)$$

If we square the first term and neglect higher powers, then

$$P = \left[r^2\left(1 - \frac{y^2 + z^2}{r^2} - \frac{(y^2 + z^2)^2}{4r^4} - \frac{(\eta^2 + \xi^2)}{Rr} - \frac{(\eta^2 + \xi^2)^2}{4rR^3}\right.\right.$$
$$\left. + \frac{(y^2 + z^2)^2}{4r^4} + \frac{(\eta^2 + \xi^2)^2}{4R^2r^2} + \frac{(y^2 + z^2)(\eta^2 + \xi^2)}{2Rr^3}\right)$$
$$\left. + (y^2 + z^2) - 2(y\xi + z\eta) + (\xi^2 + \eta^2) \right]^{1/2} \quad (13)$$

$$P = r\left[1 + \frac{(\xi^2 + \eta^2)}{r}\left(\frac{1}{r} - \frac{1}{R}\right) - \frac{2}{r^2}(y\xi + z\eta)\right.$$

$$\left. + \frac{(\eta^2 + \xi^2)^2}{4rR^2}\left(\frac{1}{r} - \frac{1}{R}\right) + \frac{(y^2 + z^2)(\eta^2 + \xi^2)}{2Rr^3}\right]^{1/2} \tag{14}$$

$$P = r\left[1 + \frac{(\xi^2 + \eta^2)}{2r}\left(\frac{1}{r} - \frac{1}{R}\right) - \frac{(y\xi + z\eta)}{r^2}\right.$$

$$+ \frac{(\eta^2 + \xi^2)^2}{8rR^2}\left(\frac{1}{r} - \frac{1}{R}\right) + \frac{(y^2 + z^2)(\eta^2 + \xi^2)}{4Rr^3}$$

$$- \frac{(\xi^2 + \eta^2)^2}{8r^2}\left(\frac{1}{r} - \frac{1}{R}\right)^2 - \frac{(y\xi + z\eta)^2}{2r^4}$$

$$\left. + \frac{(\xi^2 + \eta^2)}{2r^3}(y\xi + z\eta)\left(\frac{1}{r} - \frac{1}{R}\right)\right] \tag{15}$$

$$P = r - \frac{(y\xi + z\eta)}{r} + \frac{(\xi^2 + \eta^2)}{2}\left(\frac{1}{r} - \frac{1}{R}\right)$$

$$+ \frac{(\eta^2 + \xi^2)^2}{8}\left(\frac{1}{r} - \frac{1}{R}\right)\left(\frac{1}{R^2} - \frac{1}{r^2} + \frac{1}{rR}\right)$$

$$+ \frac{(\xi^2 + \eta^2)}{2r^2}(y\xi + z\eta)\left(\frac{1}{r} - \frac{1}{R}\right)$$

$$+ \frac{(y^2 + z^2)(\eta^2 + \xi^2)}{4Rr^2} - \frac{(y\xi + z\eta)^2}{2r^3} \tag{16}$$

In order to find the total path length between any two points in object and image space, it is necessary to substitute the appropriate x_1, y_1, and r_1 into equation (10), thereby determining P_1 and then similarly determining P_2. The result is

$$P = r_1 + r_2$$

$$- \xi\left(\frac{y_1}{r_1} + \frac{y_2}{r_2}\right) - \eta\left(\frac{z_1}{r_1} + \frac{z_2}{r_2}\right)$$

$$+ \frac{(\xi^2 + \eta^2)}{2}\left(\frac{1}{r_1} + \frac{1}{r_2} - \frac{2}{R}\right)$$

$$- \frac{(\xi^2 + \eta^2)^2}{8}\left(\frac{2}{R^3} + \frac{1}{r_1^3} + \frac{1}{r_2^3} - \frac{2}{r_1^2 R} - \frac{2}{r_2^2 R}\right)$$

$$+ \frac{(\xi^2 + \eta^2)}{2}\left[\frac{(y_1\xi + z_1\eta)}{r_1^2}\left(\frac{1}{r_1} - \frac{1}{R}\right) + \frac{(y_2\xi + z_2\eta)}{r_2^2}\left(\frac{1}{r_2} - \frac{1}{R}\right)\right]$$

$$+ (\xi^2 + \eta^2)\left(\frac{y_1^2 + z_1^2}{4Rr_1^2} + \frac{y_2^2 + z_2^2}{4Rr_2^2}\right) - \frac{1}{2}\left[\frac{(y_1\xi + z_1\eta)^2}{r_1^3} + \frac{(y_2\xi + z_2\eta)^2}{r_2^3}\right] \quad (17)$$

The first term is a constant and is therefore not an aberration. If the angle of incidence equals the angle of diffraction in the $x\xi$-plane, then $\frac{y_1}{r_1} = -\frac{y_2}{r_2}$ and the first part of the second term equals zero. The second portion of the second term is a linearly increasing path difference normal to the grating lines which is responsible for the dispersion in a grating system and is therefore not considered an aberration either. The third term expresses the effect of defocussing. In general the focal plane is curved. The fourth term is spherical aberration and the fifth is coma. Both of these terms can be simplified somewhat using the relation $\left(\frac{1}{r_1} + \frac{1}{r_2} - \frac{2}{R} = 0\right)$. The last term is astigmatism and may also be simplified by collecting like terms in ξ^2, $\eta^2 + \xi\eta$. After simplification

$$\Delta P_{defocus} = \frac{(\xi^2 + \eta^2)}{2} \left(\frac{1}{r_1} + \frac{1}{r_2} - \frac{2}{R} \right) \tag{18}$$

$$\Delta P_{sph} = - \frac{(\xi^2 + \eta^2)^2}{4R} \left(\frac{1}{R} - \frac{1}{r_1} \right)^2 \tag{19}$$

$$\Delta P_{coma} = \frac{(\xi^2 + \eta^2)}{2} \cdot \left(\frac{1}{r_1} - \frac{1}{R} \right) \left[\frac{(y_1 \xi + z_1 \eta)}{r_1^2} - \frac{(y_2 \xi + z_2 \eta)}{r_2^2} \right] \tag{20}$$

$$\Delta P_{ast} = \xi^2 \left(\frac{y_1^2 + z_1^2}{4R r_1^2} + \frac{y_2^2 + z_2^2}{4R r_2^2} - \frac{y_1^2}{2r_1^3} - \frac{y_2^2}{2r_2^3} \right)$$

$$- \xi\eta \left(\frac{y_1 z_1}{r_1^3} + \frac{y_2 z_2}{r_2^3} \right)$$

$$+ \eta^2 \left(\frac{y_1^2 + z_1^2}{4R r_1^2} + \frac{y_2^2 + z_2^2}{4R r_2^2} - \frac{z_1^2}{2r_1^3} - \frac{z_2^2}{2r_2^3} \right) \tag{21}$$

If we consider the first and second gratings independently and use a central wavelength to calculate the aberrations, then the results are as listed in Table 2.

The largest aberration is astigmatism on the second grating resulting from the $\xi\eta$ astigmatism term. This is followed by ξ^2 astigmatism from the first grating and then by η coma from the first grating. In general astigmatism is a cylindrical deformation that causes the focus of the wavefront to vary. It is therefore possible to correct the astigmatism at any one point in the focal plane by introducing a cylindrical or toric surface somewhere in the optical system.

TABLE 2

PRINCETON ADVANCED SATELLITE SPECTROGRAPH
OPTICAL PATH DIFFERENCES

Parameter	* First Grating	Second Grating
R	96.43	∞
r_1	51.43	-735.0
r_2	771.43	735.0
y_1/r_1 ($\sin\beta$)	0.0	-0.3185
y_2/r_2 ($\sin\beta'$)	0.0	-0.3185
z_1/r_1 ($\sin\gamma$)	-0.03108	0.09772
z_2/r_2 ($\sin\gamma'$)	0.06674	-0.09772
$\xi_{max}=\eta_{max}=(\xi^2+\eta^2)^{1/2}{}_{max}$	2.571	2.45
ΔP_{sph}	-0.00000939	0.0
$\Delta P_{coma\xi}$	0.0	-0.00000867
$\Delta P_{coma\eta}$	-0.00005325	0.0
$\Delta P_{ast\xi^2}$	0.0000928	0.0
$\Delta P_{ast\xi\eta}$	0.0	-0.0002541
$\Delta P_{ast\eta^2}$	-0.0000117	0.0

Balancing aberrations on one surface with those on another is out of the question with the present geometry since none of the aberrations have contributions from both surfaces. In theory it should also be possible to correct coma at any point in the focal plane with a surface having a cubic term to describe the sag. Such a surface would be difficult to make because of the lack of symmetry and would also necessitate major changes to the computer program used in optical design. A similar limitation prevents any serious consideration of the theoretical possibility of correcting two aberrations, such as spherical aberration and coma, over the entire field using all the freedom inherent with two surfaces.

The surface required to correct the $\xi\eta$ astigmatism term is a toric surface with its axis at 45 degrees to the y- and z-axes. This can be shown by expanding the sag of such a surface in a series such as follows

$$\text{Sag} = \frac{(\eta^2 + \xi^2)\,(c_1 + c_2)}{4} + \frac{\xi\eta(c_1 - c_2)}{2} \tag{22}$$

where c_1 and c_2 are the curvatures of the major and minor axes at 45 degrees to the η- and ξ-axes.

The first term in this expansion is the sag associated with any spherical surface. The second term, which has the required $\xi\eta$ dependency, is due to the astigmatic nature of a toroidal surface. In theory, the toric surface could be placed on either of the two grating surfaces; but, from a manufacturing point of view, it is desirable to place it on the predisperser thus leaving the echelle flat. The difference in curvatures on the predisperser can be calculated from equation (22) by assuming that the OPD is twice the variation in sag, which is strictly true for normal incidence only. Thus, from Table 2 and equation (22).

$$\xi\eta\,(c_1 - c_2) = 0.0002541$$

$$c_1 - c_2 = \frac{(0.0002541)}{\dfrac{(2.571)^2}{2}}$$

$$= 0.000077$$

This agrees quite well with the 0.0000809 value found by trial and error using the computer. The next largest aberration is astigmatism from the first grating in the ξ- or y-direction. This could also be remedied by a toroidal surface, but it is more conveniently corrected simply by adjusting the focus to coincide with the astigmatic image plane in the high resolution or ξ-direction. The only remaining aberration of any appreciable magnitude is coma from the first grating. Coma correction would require a non-symmetrical figure (cubic sag term) that would be very difficult to generate; so coma correction was not attempted.

SECTION V

CONCLUSIONS

A two-element echellé spectrograph covering the spectral region from 1000Å to 2800Å on a single 36-mm-diameter vidicon format is feasible. In a design that uses only a flat echelle grating and a slightly astigmatic spherical primary, all the aberrations can be kept sufficiently small so as to render the system essentially diffraction-limited at the f/150 focal plane. In order to keep the dispersion suitably high, it is neccessary to knock a few corners off of the spectrum at the long wavelength end, but this need not eliminate any of the more important interstellar absorption lines. The resolution likely to be achieved with such an instrument will probably depend more on the scattered light level and the optical perfection of the gratings than on the aberrations inherent in such a system. However, considering only the combined effects of diffraction and the optical aberrations, then a limiting resolution of 20 lines per millimeter should be possible below 3000Å. This corresponds to a resolution of about one part in 10^4.

It is therefore recommended that construction of the breadboard instrument proceed and that the optical efficiencies and scattered light levels be measured.